Characterization of a cysteine-less human reduced folate carrier: localization of a substrate-binding domain by cysteine-scanning mutagenesis and cysteine accessibility methods

Wei CAO* and Larry H. MATHERLY*†[1]

*Department of Pharmacology, Wayne State University School of Medicine, 540 East Canfield Avenue, Detroit, MI 48201, U.S.A., and †Experimental and Clinical Therapeutics Program, Barbara Ann Karmanos Cancer Institute, Wayne State University School of Medicine, 110 E. Warren Avenue, Detroit, MI 48201, U.S.A.

The human reduced folate carrier (hRFC) mediates the transport of reduced folates and classical anti-folates into mammalian cells. Whereas the functionally important domains in hRFC are poorly characterized, previous studies with anti-folate-resistant cells suggest critical roles for transmembrane domain (TMD) 1 and residues (Gly^{44}, Glu^{45}, Ser^{46} and Ile^{48}) in or flanking this region. An hRFC mutant devoid of cysteine residues was prepared by deleting the C-terminal 56 amino acids, including four cysteine residues, and mutagenizing the remaining cysteine residues to serine residues. A fully functional cysteine-less hRFC protein was expressed in transport-impaired MtxRIIOua^{R}2-4 Chinese-hamster ovary cells. To explore the role of residues in or flanking TMD1 in transport, all 24 amino acids from Trp^{25} to Ile^{48} of hRFC were mutated individually to cysteine residues, and the mutant hRFCs were transfected into MtxRIIOua^{R}2-4 cells. All of the 24 cysteine mutants were expressed and, with the exception of R42C ($Arg^{42} \rightarrow Cys$), were capable of mediating methotrexate uptake above the low level in MtxRIIOua^{R}2-4 cells. We found that by treating the transfected cells with the small, water-soluble, thiol-reactive anionic reagent, sodium (2-sulphonatoethyl) methanethiosulphonate, methotrexate transport by several of the cysteine-substituted hRFC mutants was significantly inhibited, including Q40C, G44C, E45C and I48C. Sodium (2-sulphonatoethyl) methanethiosulphonate transport inhibition of the Q40C, G44C and I48C mutants was protected by leucovorin [(6*R*,*S*)-5-formyltetrahydrofolate], indicating that these residues lie at or near a substrate-binding site. Using surface-labelling reagents [*N*-biotinylaminoethyl methanethiosulphonate and 3-(*N*-maleimidylpropionyl)biocytin, combined with 4-acetamido-4′-maleimidylstilbene-2,2′-disulphonic acid] with cysteine mutants from positions 37–48, the extracellular TMD1 boundary was found to lie between residues 39 and 40, and amino acids 44–46 and 48 were localized to the TMD1 exofacial loop. Collectively, our results imply that amino acids 40, 44, 48 and, possibly, 42 serve important roles in hRFC transport, albeit not as structural components of the putative transmembrane channel for folate substrates.

Key words: folate, methanethiosulphonate, methotrexate, *N*-biotinylaminoethyl methanethiosulphonate, 3-(*N*-maleimidylpropionyl)biocytin, transporter.

INTRODUCTION

Reduced folates are essential cofactors required for the *de novo* biosynthesis of purine nucleotides, thymidylate and serine and methionine residues in mammalian cells, for which they function as donors of single-carbon units [1]. Folate deficiency contributes to chromosomal instability, resulting in malignant transformation [2]. Moreover, folate deficiency also plays an important role in foetal abnormalities [3] and in the development of cardiovascular disease [4]. As hydrophilic anionic molecules, natural folates show only minimal capacities to cross biological membranes by diffusion alone. Accordingly, sophisticated membrane transport systems have evolved to facilitate membrane translocation of these cofactors. The reduced folate carrier (RFC) is expressed ubiquitously in tissues and tumours [5] and has long been recognized as the major membrane transporter for reduced folates in mammalian cells [6–10]. RFC levels are also critical determinants of the anti-tumour activities of anti-folate drugs such as methotrexate (Mtx) and Raltitrexed (Tomudex), and impaired transport is a frequent mechanism of anti-folate resistance [7–10]. Furthermore, alterations in the levels and/or function of the human RFC (hRFC) have been described previously in clinical specimens from patients treated with Mtx [11–13].

hRFC cDNAs were cloned in 1995 [14–17] and, from the nucleotide sequence, they encode a protein with 591 amino acids. Hydropathy analysis predicts up to 12 TMDs, composed of stretches of mostly hydrophobic, α-helix-promoting amino acids, internally orientated N- and C-termini and a single outwardly facing N-glycosylation consensus site at position 58 [6,7]. The latter appears to be heavily glycosylated, so that hRFC protein appears as a broadly migrating band of approx. 85–92 kDa on Western blots [7,14].

Despite extensive studies to characterize the functional properties of the RFC protein, surprisingly little is known about the amino acid residues or domains that are actually important to binding and/or membrane translocation of anionic folate and anti-folate substrates. However, insights into these features can be gleaned by characterizing the molecular alterations in RFC accompanying resistance to anti-folates after selection with

Abbreviations used: biotin maleimide, 3-(*N*-maleimidylpropionyl)biocytin; CHO, Chinese-hamster ovary; RFC, reduced folate carrier; hRFC, human RFC; leucovorin, (6*R*,*S*)-5-formyltetrahydrofolate; MTS, methanethiosulphonate; MTSEA, 2-aminoethyl methanethiosulphonate hydrobromide; MTSEA-biotin, *N*-biotinylaminoethyl methanethiosulphonate; MTSES, sodium (2-sulphonatoethyl) methanethiosulphonate; MTSET, 2-(trimethylammonium)ethyl methanethiosulphonate bromide; Mtx, methotrexate; stilbenedisulphonate maleimide, 4-acetamido-4′-maleimidylstilbene-2,2′-disulphonic acid; TMD, transmembrane domain; for brevity the one-letter system for amino acids has been used: R42C, for example, means $Arg^{42} \rightarrow Cys$.

[1] To whom correspondence should be addressed at Experimental and Clinical Therapeutics Program (e-mail matherly@karmanos.org).

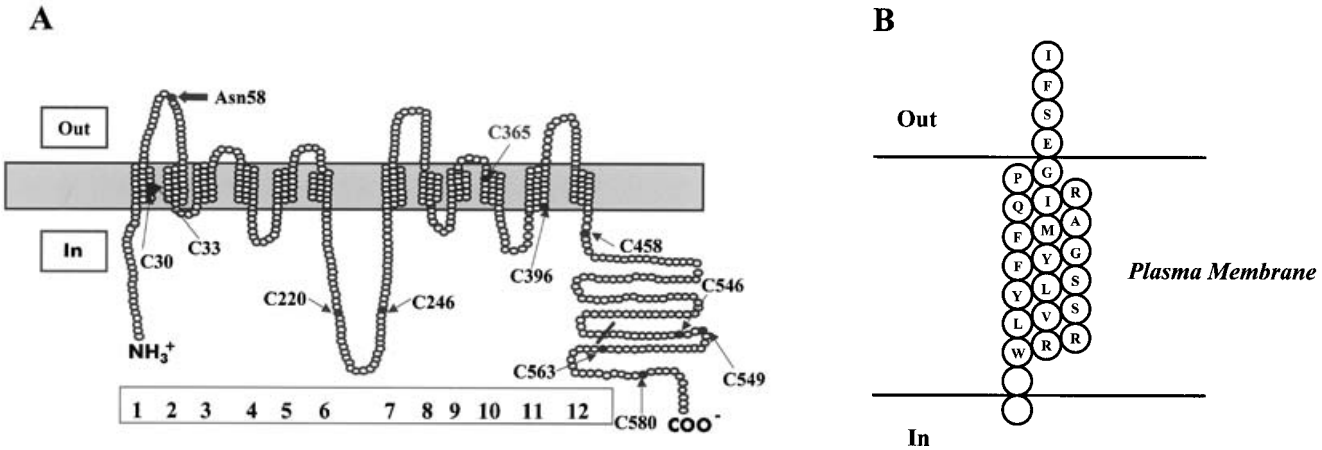

Figure 1 Membrane topology of hRFC and the location of cysteine residues

(**A**) Topology model for hRFC (TMPred [48]), depicting 12 TMDs, internally orientated N- and C-termini and an externally orientated N-glycosylation site at Asn[58]. Also shown are the positions of the 11 endogenous cysteine residues in the hRFC primary sequence. All the mutant constructs used in the present study were truncated (position indicated by the black bar) without the C-terminal 56 amino acids, which include four cysteine residues. (**B**) An expanded schematic of TMD1 shows the predicted positions of the Trp[25]–Ile[48] stretch of amino acids targeted for cysteine-scanning mutagenesis.

anti-folate drugs or site-directed mutagenesis. Most notable are residues in or flanking transmembrane domain 1 (TMD1), for which mutations in highly conserved residues are accompanied by profound effects on transport substrate binding (e.g. Gly[44] [18,19], Glu[45] [20–22] and Ile[48] [23]) or rates of carrier translocation (Ser[46] [24]).

The advent of thiol reagents with reactivities amenable to use with intact cells, typified by the alkylthiosulphonates sodium (2-sulphonatoethyl) methanethiosulphonate (MTSES), 2-(trimethylammonium)ethyl methanethiosulphonate bromide (MTSET) and 2-aminoethyl methanethiosulphonate hydrobromide (MTSEA) [25,26], has revolutionized the structural analysis of membrane-spanning ion channels and transporters. Thus, by reinserting cysteine residues into functional 'cysteine-less' proteins and by treating transfected cells with cysteine-reactive agents, it is possible to elucidate membrane topologies [27–32], identify amino acids that are aqueous accessible [33–40], and also determine spatial relationships between TMDs [41,42]. Of particular interest is the use of cysteine-reactive agents with cysteine-substituted accessibility methods in which patterns of cysteine reactivity in singly substituted cysteine mutants can be used to map the ligand-binding domains of membrane proteins [43,44]. Variations of this approach have been elegantly applied to characterize the structures of an assortment of membrane proteins such as *Escherichia coli* lactose permease [45], prostaglandin transporter [46], glucose transporter Glut1 [29], human dopamine transporter [47] and *p*-glycoprotein [35], as well as ion channels [43].

hRFC contains 11 cysteine residues (Figure 1). Although the structural or functional importance of cysteine residues in RFC transport has not been tested directly, the mouse RFC was reported previously to be inhibited by the organomercurial, *p*-chloromercuribenzoate [49]. In the present study, we further examine the role of cysteine residues in hRFC transport by expressing a functional hRFC protein devoid of cysteine residues. We use cysteine-scanning mutagenesis of the 'cysteine-less' hRFC in conjunction with thiol-reactive *N*-biotinylaminoethyl methanethiosulphonate (MTSEA-biotin), 3-(*N*-maleimidylpropionyl)biocytin (referred to hereafter as biotin maleimide) and MTSES reagents to explore the roles of residues in or flanking TMD1 in hRFC transport. Our results imply that amino acids 40, 44, 48 and, possibly, 42 serve important roles in hRFC transport, albeit not as structural components of the putative transmembrane channel for folate substrates.

MATERIALS AND METHODS

Reagents

[3′,5′,7–^{3}H]Mtx (20 Ci/mmol) was purchased from Moravek Biochemicals (Brea, CA, U.S.A.). Unlabelled Mtx and (6*R*,*S*)-5-formyltetrahydrofolate (referred to hereafter as leucovorin) were provided by the Drug Development Branch, National Cancer Institute, National Institutes of Health (Bethesda, MD, U.S.A.). Both labelled and unlabelled Mtx were purified before use, as described previously [50]. MTSES, MTSEA and MTSET were purchased from Anatrace (Maumee, OH, U.S.A.). MTSEA-biotin was purchased from Toronto Research Chemicals (Toronto, ON, Canada). Biotin maleimide and 4-acetamido-4′-maleimidylstilbene-2,2′-disulphonic acid (referred to hereafter as stilbenedisulphonate maleimide) were purchased from Molecular Probes (Eugene, OR, U.S.A.). Protein G-plus agarose beads were purchased from Santa Cruz Biotechnology (Santa Cruz, CA, U.S.A.). Restriction enzymes and other molecular biological products were from Promega (Madison, WI, U.S.A.) or Invitrogen (Carlsbad, CA, U.S.A.) or Roche (Indianapolis, IN, U.S.A.). Tissue culture reagents and supplies were purchased from assorted vendors with the exception of iron-supplemented calf serum and dialysed foetal bovine serum, which were purchased from Hyclone Technologies (Logan, UT, U.S.A.) and Life Technologies (Gaithersburg, MD, U.S.A.) respectively. Synthetic oligonucleotides were purchased from Invitrogen.

Cell culture

Transport-defective Mtx-resistant Chinese-hamster ovary (CHO) cells, MtxRIIOua^{R}2-4 [51], were a gift from Dr Wayne Flintoff (Department of Microbiology and Immunology, University of Western Ontario, London, ON, Canada). MtxRIIOua^{R}2-4 cells were grown in α-minimal essential medium with 10% (v/v) iron-supplemented bovine calf serum, penicillin (100 units/ml)

Table 1 PCR primers for preparing hRFC^{his6} *Cys-less* and cysteine-substituted hRFC^{his6} mutant constructs

Mutation	Forward mutation primer	Reverse mutation primer
C33S	CTCGTGTGCTACCTTAGCTTCTACGGCTTCATGG	CATGAAGCCGTAGAAGCTAAGGTAGCACACGAG
C246S	GCCCTGCGGGTGGCCTCTGGGGACTCAGTGCTG	CAGCACTGAGTCCCCAGAGGCCACCCGCAGGGC
C396S	CTGTCTAAAGAGCTCTCTGCCCTGGTCTTCGGG	CCCGAAGACCAGGGCAGAGAGCTCTTTAGACAGA
C30S/C33S	CGCCTCGTGTCCTACCTTAGCTTCTACGGCTTC	GAAGCCGTAGAAGCTAAGGTAGGACACGAGGCG
C220S	GCGGTCAGAAACCTCGGCTTCGGAGCTG	CAGCTCCGAAGCCGAGGTTTCTGACCGC
C365S	CTGTCCTATGCGGCCTTCGTGCTGTTC	GAACAGCACGAAGGCCGCATAGGACAGC
C458S	CTGGATGGCCTGCGGCACTCACAGCG	CGCTGTGAGTGCCGCAGGCCATCCAG
W25C	CTCCGGTCCTGCCGACGCCTCGTG	CACGAGGCGTCGGCAGGACCGGAG
R26C	CGGTCCTGGTGCCGCCTCGTGTCC	GGACACGAGGCGGCACCAGGACCG
R27C	CGGTCCTGGCGGTGCCTCGTGTCC	GGACACGAGGCACCGCCAGGACCG
L28C	TCCTGGCGACGCTGCGTGTCCTAC	GTAGGACACGCAGCGTCGCCAGGA
V29C	TCCTGGCGACGCCTCTGCTCCTACCTTAGC	GCTAAGGTAGGAGCAGAGGCGTCGCCAGGAC
S30C	CTCGTGTGCTACCTTAGCTTCTAC	GTAGAAGCTAAGGTAGCACACGAG
Y31C	CTCGTGTCCTGCCTTAGCTTCTAC	GTAGAAGCTAAGGCAGGACACGAG
L32C	GTGTCCTACTGTAGCTTCTACGGCTTCATG	CATGAAGCCGTAGAAGCTACAGTAGGACAC
S33C	CTACCTTTGCTTCTACGGCTTCATGG	CCATGAAGCCGTAGAAGCAAAGGTAG
F34C	TACCTTAGCTGCTACGGCTTCATGG	CCATGAAGCCGTAGCAGCTAAGGT
Y35C	CTTAGCTTCTGCGGCTTCATGGC	GCCATGAAGCCGCAGAAGCTAAG
G36C	CTTCTACTGCTTCATGGCACAGAT	ATCTGTGCCATGAAGCAGTAGAAG
F37C	CTTCTACGGCTGCATGGCACAGATAC	GTATCTGTGCCATGCAGCCGTAGAAG
M38C	CTACGGCTTCTGCGCTCAGATTCGGC	GCCGAATCTGAGCGCAGAAGCCGTAG
A39C	CTTCATGTGTCAGATACGTCCAGGGG	CCCCTGGACGTATCTGACACATGAAG
Q40C	CTTCATGGCGTGTATACGTCCAGGG	CCCTGGACGTATACACGCCATGAAG
I41C	CATGGCTCAGTGTCGACCAGGGGAGAG	CTCTCCCCTGGTCGACACTGAGCCATG
R42C	GCAGATATGTCCAGGGGAGAGCTTC	GAAGCTCTCCCCTGGACATATCTGC
P43C	CAGATACGGTGTGGGGAGAGCTTCATC	GATGAAGCTCTCCCCACACCGTATCTG
G44C	CAGATACGGCCATGTGAGAGCTTCATCACC	GGTGATGAAGCTCTCACATGGCCGTATCTG
E45C	GATACGGCCAGGGTGTAGCTTCATCACC	GGTGATGAAGCTACACCCTGGCCGTATC
S46C	GAGTGCTTCATCACCCCCTACCTC	GAGGTAGGGGGTGATGAAGCACTC
F47C	GAGAGCTGCATCACCCCCTACCTC	GAGGTAGGGGGTGATGCAGCTCTC
I48C	GAGAGCTTCTGCACCCCCTACCTC	GAGGTAGGGGGTGCAGAAGCTCTC

and streptomycin (100 μg/ml). The pC43/10 CHO cell line was derived from MtxRIIOua^{R}2-4 cells by transfection with the full-length wild-type hRFC cDNA (pC43), as described previously [14], and maintained in complete medium in the presence of 1.5 mg/ml G418. CHO cells were grown as monolayers for transfection and cytotoxicity assays; for transport experiments, cells were grown in suspension in spinner flasks.

Site-directed mutagenesis

An hRFC^{his6} construct containing a truncated hRFC with seven of the 11 cysteine residues and including both c-*myc* and his6 epitopes on the hRFC C-terminus was prepared by subcloning 1607 bp of an hRFC coding sequence (prepared by *Eco*RI digestion of the full-length hRFC in pBluescript SK [14]) into pcDNA3.1(−) myc-his A expression vector (Invitrogen) at the *Bam*HI and *Xho*I restriction sites (designated hRFC^{his6}*wt*). To prepare the hRFC^{his6}*Cys-less*, all seven of the remaining cysteine residues (Cys^{30}, Cys^{33}, Cys^{220}, Cys^{246}, Cys^{365}, Cys^{396} and Cys^{458}) in hRFC^{his6}*wt* were replaced individually with serine residues by PCR mutagenesis using an overlap-extension protocol [52,53].

The hRFC construct containing three conserved cysteine mutations, C33S, C246S and C396S, was first prepared. To generate the hRFC fragments containing C33S or C246S, two PCR steps were performed to amplify two separate products, using forward mutation primers (see Table 1) and the rHA7 primer (5′-CTCGTTCCACAGGATGTGCAC-3′; positions 882–862, relative to the ATG start codon, where A is number 1), or reverse mutation primers (Table 1) and the p8 primer (5′-CAGTGTCACCTTCGTCCCCTCCG-3′; positions −46 to −24). The full-length pC43 construct was used as a template. PCR conditions for the primary PCRs were 94 °C for 30 s, 56 °C for 30 s and 72 °C for 45 s. Secondary PCRs were performed with the p8/rHA-7 primers and the mixed primary PCR products as templates. The same strategy and PCR conditions were used to prepare the C396S fragment. KS2 (5′-CGCAGCCTCTTCTTCAACCGC-3′; positions 622–642) and RFCout12 (5′-GACAACCCCTTCCCCCTGCACTCTGT-3′; positions 1647–1619) primers were used with the corresponding reverse and forward mutation primers respectively (Table 1), and pC43 hRFC template for the primary PCR. Secondary PCR was performed using KS2/RFCout12 and the mixed primary PCR products as template. The C33S, C246S and C396S mutant amplicons were digested with *Bbr*PI–*Apa*I, *Apa*I–*Not*I and *Not*I–*Sfi*I respectively, and the digested products purified and ligated into the *Bbr*PI- and *Sfi*I-digested hRFC^{his6}*wt* cDNA in pcDNA3.1 to generate the hRFC^{his6}3C/S construct.

Using the hRFC^{his6}3C/S construct as template, the fragments containing C30S, C220S or C365S were generated by an analogous two-step PCR with complementary mutagenesis primers (Table 1) and the respective upstream (P8) and downstream (CW9, 5′-GGGCCAGGTATGGGTCGCTCTGTCTCTG-3′; positions 1674–1647) primers. PCR conditions were identical with those described above. The C30S, C220S and C365S mutant amplicons were digested with *Bbr*PI–*Apa*I, *Apa*I–*Not*I and *Not*I–*Sfi*I respectively, and the digested products purified and ligated into the *Bbr*PI- and *Sfi*I-digested hRFC^{his6}3C/S in pcDNA3.1 to generate hRFC^{his6}6C/S.

Finally, to construct the hRFC^{his6}*Cys-less* product, the fragment containing C458S was generated by the same strategy using the complementary mutagenic primers (shown in Table 1) and the KS2/CW9 primers, with hRFC^{his6}6C/S as template. PCR

conditions were identical with those described above. After digestion with *Not*I and *Sfi*I, the product was ligated into the *Not*I- and *Sfi*I-digested hRFC^{his6}6C/S.

hRFC^{his6}*Cys-less* in pcDNA3.1 was employed as template with overlap-extension PCR to generate the single cysteine-replacement mutant constructs in which each residue from Trp^{25} to Ile^{48} was replaced individually by a cysteine residue. The complementary mutagenesis primers (Table 1) were used with the upstream P8 and downstream rHA7 primers. The amplicons carrying the single cysteine substitutions were digested with *Bbr*PI and *Not*I, and ligated into the *Bbr*PI–*Not*I-digested hRFC^{his6}*Cys-less* construct.

All mutations were confirmed by DNA sequencing.

Cell transfections and selection of stable transfectants

hRFC^{his6}*wt*, hRFC^{his6}*Cys-less* and the 24 single cysteine-substituted hRFC^{his6} constructs were transfected into transport-defective MtxRIIOua^{R}2-4 CHO cells with polybrene [14], reflecting their amenability to 'high throughput' expression and screening. Clones were selected with 1.5 mg/ml G418, and G418-resistant clones were isolated and expanded. Stable transfectants were initially screened for Mtx sensitivities by plating at low densities (10000 cells/ml) in complete medium with dialysed foetal bovine serum and 0, 10, 50 or 200 nM Mtx. Clones exhibiting restored Mtx sensitivities compared with MtxRIIOua^{R}2-4 cells were assayed for [^{3}H]Mtx uptake (see below) and hRFC expression on Western blots.

Western-blot analysis of hRFC transfectants

Plasma membranes were prepared by differential centrifugation, as described previously [54]. Membrane proteins were electrophoresed in the presence of (7.5 % gel) as described by Laemmli [55] and electroblotted on to PVDF membranes (Pierce, Rockland, IL, U.S.A.) [56]. Protein loading was confirmed by staining the PVDF membranes with 0.1 % Coomassie Blue. Immunoreactive hRFC proteins were detected by enhanced chemiluminescence (Roche) with Protein A-purified hRFC-specific antibody, generated in rabbits with a glutathione S-transferase–hRFC fusion protein [18], and images were recorded on X-ray film. The relative amounts of immunoreactive proteins were determined by scanning densitometry, using a Kodak Digital Science 440CF Image Station.

Immunofluorescence microscopy

Approx. 5×10^6 cells were washed twice with PBS, fixed with 3.3 % (w/v) paraformaldehyde/PBS for 30 min on ice and permeabilized with 0.1 % Triton X-100 for 5 min at 4 °C. After extensive washing with PBS, cells were blocked with 1 % BSA/PBS for 1 h at 4 °C. The hRFC^{his6} proteins were detected using monoclonal anti-his antibody (Invitrogen), followed by incubation with a secondary goat anti-mouse IgG conjugated with Alexa Fluor 488 (Molecular Probes) at 4 °C in the dark. After extensive washing with PBS, approx. 50000 cells were cytocentrifuged on to microscope slides, mounted with a drop of 'SlowFade' anti-fade reagent (Molecular Probes) and sealed with coverslips. Detection was done with a Zeiss laser scanning microscope 310 using a ×63 water-immersion lens to image the fluorescently labelled samples.

Transport assays

Uptakes of 1 μM [^{3}H]Mtx were assayed as described previously [14,53]. Levels of intracellular radioactivity were expressed as pmol/mg of protein, calculated from direct measurements of the radioactivity and protein contents of cell homogenates. Protein assays were performed by the method of Lowry et al. [57]. Kinetic analyses involved assays of the influx rates for 180 s over the range of 0.4–4 μM [^{3}H]Mtx; kinetic constants K_t and V_{max} were calculated from Lineweaver–Burk plots.

MTSES modification and substrate protection experiments

Cells (approx. 2×10^7 cells) in suspension in 1 ml of PBS were treated with MTSES (1 mM final; prepared as a 40× concentrated aqueous stock) at 37 °C for 15 min. Reactions were terminated by dilution (10-fold) and washing four times with 10 ml of ice-cold PBS. [^{3}H]Mtx uptake was assayed for 10 min at 37 °C. To assess the effects of an hRFC substrate on MTSES inhibition, leucovorin (300 μM final concentration) was added 5 min before adding the MTSES reagent.

Detection of the TMD1-loop boundary with MTSEA-biotin and biotin maleimide/stilbenedisulphonate maleimide

Two approaches were used for mapping the TMD1-loop boundary region. (i) CHO cells (1×10^7 cells) growing in 100 mm dishes expressing hRFC^{his6}*Cys-less* and the F37C, M38C, A39C, Q40C, I41C, R42C and P43C single cysteine-substituted hRFC^{his6} mutants were treated at 37 °C with 200 μM MTSEA-biotin in PBS for 4 h. (ii) G44C-, E45C-, S46C- and I48C-hRFC mutants growing in 100 mm dishes were treated with 200 μM stilbenedisulphonate maleimide (in PBS) at room temperature (23 °C) for 30 min, followed by treatment with 200 μM biotin maleimide (in PBS) or biotin maleimide alone at room temperature for 30 min. The cells were briefly treated with 14 mM 2-mercaptoethanol to remove excess reagent and then washed twice with PBS. Cells were harvested and crude plasma membranes were prepared, as described above. For immunoprecipitation, membrane proteins were solubilized in 1 ml of cell lysis buffer [50 mM Tris (pH 7.5)/150 mM NaCl/1 % Nonidet P40/0.5 % sodium deoxycholate]. The insoluble material was pelleted (12000 ***g***, 10 min) and the supernatant was precleared overnight with Protein G-plus agarose beads (Santa Cruz Biotechnology). The beads were pelleted (12000 ***g***, 20 s) and the supernatant was incubated with anti-myc antibody (Invitrogen) and fresh Protein G-plus agarose beads overnight at 4 °C. The beads were washed three times with lysis buffer containing 0.1 % Nonidet P40, and eluted with 60 μl of Laemmli sample buffer containing 2 % (w/v) SDS for Western blotting (see above). Immunodetection of biotinylated hRFC was with peroxidase-linked streptavidin and Lumi-Light^{PLUS} substrate (Roche), whereas total immunoprecipitated hRFC was detected using an hRFC-specific antibody and standard Lumi-Light substrate (Roche).

RESULTS

A cysteine-less hRFC exhibits normal membrane targeting, expression and transport function

An early report by Goldman et al. [49] showed that treatment of L1210 cells with the organomercurial, *p*-chloromercuribenzoate, potently inhibited Mtx uptake, suggesting a role for cysteine residues in transport by RFC. To explore directly the potential structural or functional roles of cysteine residues in hRFC, a cysteine-less hRFC was constructed by (i) deleting the C-terminal 56 amino acids (including Cys^{546}, Cys^{549}, Cys^{563} and Cys^{580}) and (ii) mutagenizing the remaining cysteine residues (Cys^{30}, Cys^{33},

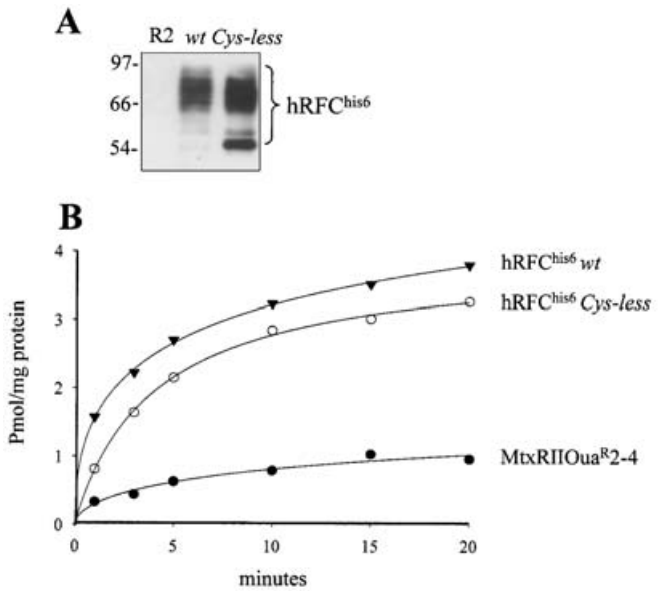

Figure 2 Expression and function of hRFC^{his6} *Cys-less* protein

(**A**) A Western blot is shown of plasma membrane proteins from MtxRIIOua^{R}2-4 CHO cells (labelled R2) and CHO transfectants stably expressing hRFC^{his6} *wt* and hRFC^{his6} *Cys-less* proteins. Proteins (20 μg) were fractionated on a 7.5 % gel in the presence of SDS and electroblotted on to a PVDF membrane. Detection was done with an anti-hRFC antibody and an enhanced chemiluminescence kit (Roche). Molecular-mass standards (in kDa) are shown on the left. (**B**) [^{3}H]Mtx (1 μM) uptake was measured for 20 min at 37 °C, as described in the Materials and methods section.

Cys^{220}, Cys^{246}, Cys^{365}, Cys^{396} and Cys^{458}) individually to serine residues by overlap-extension PCR. (Figure 1A shows a schematic of the hRFC membrane topology, including the positions of the 11 cysteine residues.) A Myc-his6 epitope was added to the hRFC C-terminus to permit immunolocalization with anti-his6 antibody, and immunoprecipitation with anti-myc antibody (see below).

Both hRFC^{his6}*wt* and hRFC^{his6}*Cys-less* constructs in pcDNA3.1 were transfected into transport-defective MtxRIIOua^{R}2-4 CHO cells. After selection with 1.5 mg/ml G418, clones were screened for carrier expression on Western blots, for membrane targeting

Table 2 Kinetic constants for Mtx influx

Cell line	K_t (μM)*	V_{max} (pmol · mg^{-1} · min^{-1})*	Normalized V_{max}†
pC43/10	1.31 ± 0.08	5.54 ± 0.19	5.54
hRFC^{his6}*wt*	0.78 ± 0.02	6.02 ± 0.23	3.34
hRFC^{his6}*Cys-less*	1.64 ± 0.26	4.17 ± 0.57	1.60

* Kinetic constants for Mtx transport were calculated by Lineweaver–Burk analysis of initial rates from three experiments as described under the Materials and methods section. K_t and V_{max} values are expressed as means ± S.E.M.

† Normalized V_{max} represents values normalized to the hRFC expression on Western blots by densitometry analysis. The expression of the full-length hRFC in pC43/10 cells [14] was given a value of 1.0 (Western blot not shown), and the normalized expressions for hRFC^{his6}*wt* and hRFC^{his6}*Cys-less* were given the values 1.8 and 2.6 respectively (Figure 2).

by confocal microscopy and for [^{3}H]Mtx uptake. Both hRFC^{his6}*wt* and hRFC^{his6}*Cys-less* were expressed at similarly high levels and migrated as approx. 65–80 kDa bands on Western blots probed with hRFC antibody (Figure 2), resembling the patterns reported previously for the full-length wild-type carrier in pC43/10 cells [14]. By confocal microscopy with anti-his antibody and Alexa 488-conjugated secondary antibody, hRFC^{his6}*wt* and hRFC^{his6}*Cys-less* proteins showed predominant plasma membrane localization (Figure 3). Finally, both hRFC^{his6}*wt* and hRFC^{his6}*Cys-less* restored Mtx uptake to MtxRIIOua^{R}2-4 CHO cells during 20 min of exposure to 1 μM [^{3}H]Mtx (Figure 2).

The kinetic constants V_{max}, K_t and V_{max}/K_t for Mtx, based on initial rates of uptake for 180 s, slightly differed among the MtxRIIOua^{R}2-4 transfectants expressing full-length wild-type hRFC (pC43/10) and the hRFC^{his6}*wt* and hRFC^{his6}*Cys-less* proteins (Table 2). Both the K_t and normalized V_{max} values (normalized for hRFC expression on Western blots) for the hRFC^{his6}*Cys-less* and hRFC^{his6}*wt* proteins varied within a 2-fold range. Although direct comparisons of normalized transport can be biased, because hRFC transport and function are not always proportional [58], we find that comparisons can be made and are reasonable for CHO transfectants with hRFC constructs, with expression levels differing within a 2–3-fold range. These results demonstrate that the characteristics of hRFC^{his6}*Cys-less* differ only slightly from those of hRFC^{his6}*wt* and strongly suggest that cysteine residues do not play major structural or functional roles in

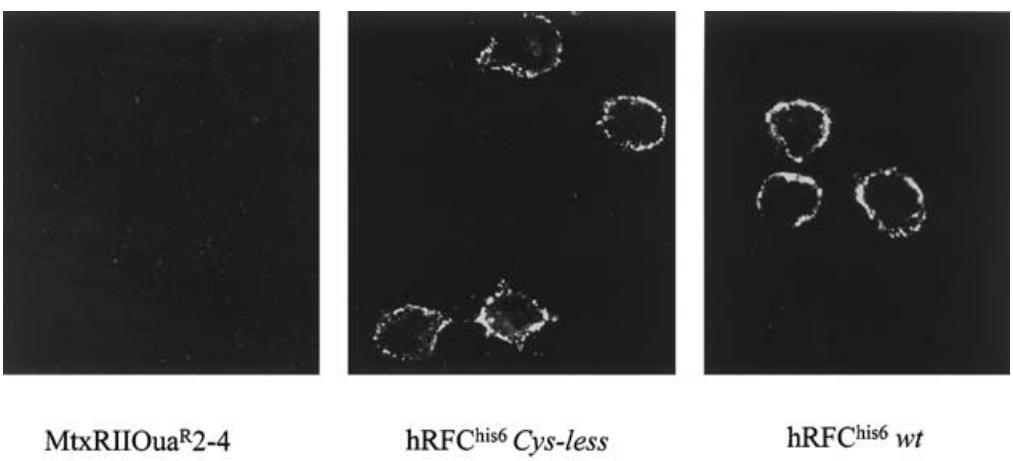

Figure 3 Confocal microscopy of CHO cells stably expressing hRFC^{his6} *wt* and hRFC^{his6} *Cys-less*

The hRFC expression for hRFC^{his6}*wt*- and hRFC^{his6}*Cys-less*-expressing cells was detected using a monoclonal anti-his6 antibody (Invitrogen), followed by incubation with a secondary goat anti-mouse IgG conjugated with Alexa Fluor 488. MtxRIIOua^{R}2-4 cells were used as negative control. Experimental details are provided in the Materials and methods section.

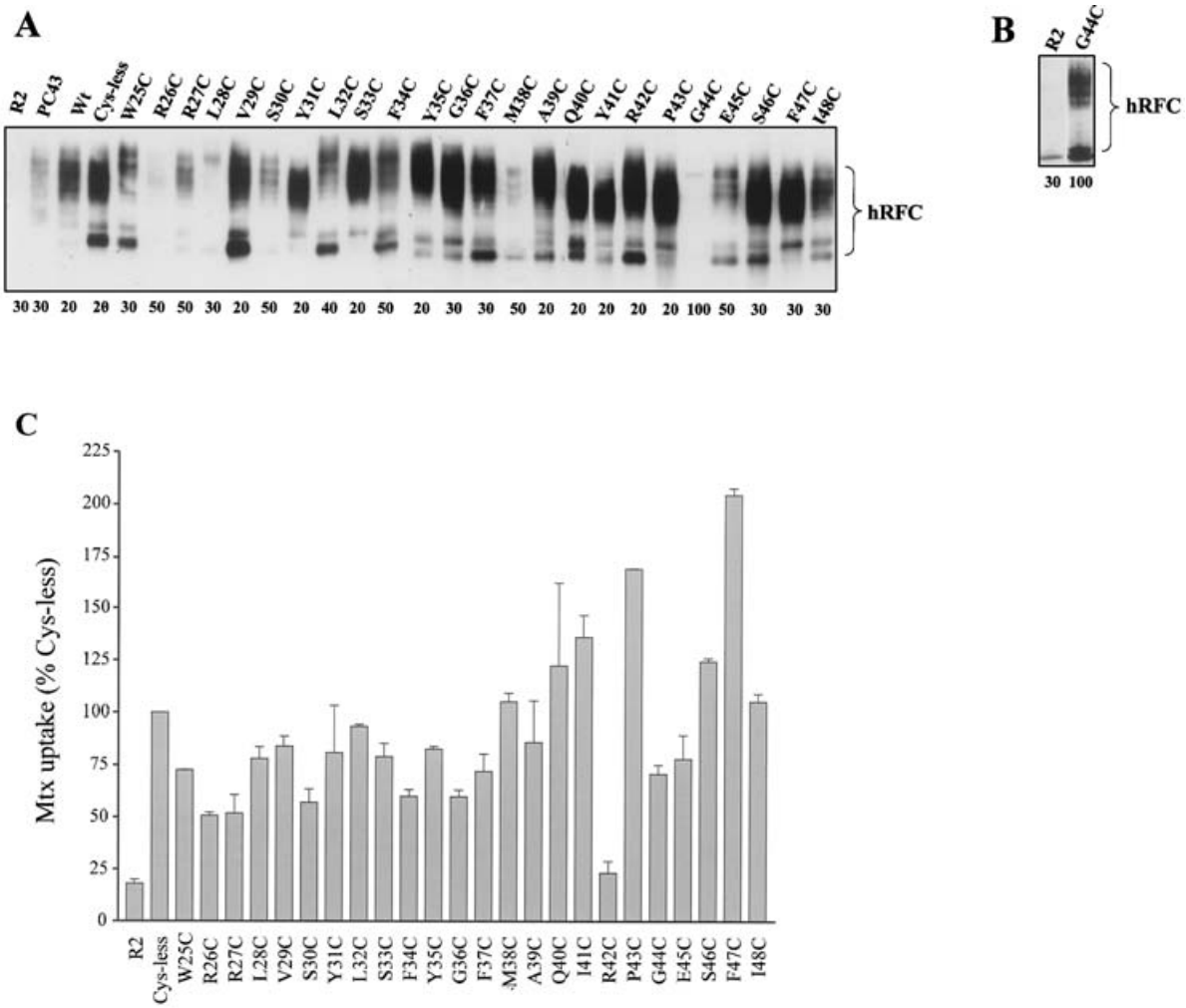

Figure 4 Expression and transport function of single cysteine-substituted hRFC^{his6} mutants

(**A**) Levels of hRFC expression on a Western blot of plasma membrane proteins from RFC-deficient CHO cells (MtxRIIOua^{R}2-4 cells; labelled 'R2') and R2 transfectants expressing full-length hRFC (pC43), hRFC^{his6} *wt* and hRFC^{his6} *Cys-less*, and single cysteine-substituted hRFC^{his6} mutants. Detection was done with anti-hRFC antibody and an enhanced chemiluminescence kit. Amounts of protein (mg) loaded in each lane are indicated. (**B**) Western-blot results for the low-expressing G44C-hRFC^{his6} after an extended exposure to film. (**C**) Results are shown for rates of [^{3}H]Mtx transport in R2 cells and R2 transfectants expressing hRFC^{his6} *Cys-less* and single cysteine-substituted hRFC^{his6} mutants. [^{3}H]Mtx (1 μM) uptakes were measured for 10 min at 37 °C. Transport results are expressed relative to the level for hRFC^{his6} *Cys-less* and are means $\pm$ S.E.M. for 2–3 separate experiments.

hRFC transport. The somewhat lower normalized V_{max} values for the hRFC^{his6} proteins compared with full-length wild-type hRFC imply a modest effect on carrier function from the loss of the C-terminal 56 amino acids.

Expression and function of single cysteine-substituted hRFC mutants

The availability of a functional hRFC^{his6} *Cys-less* construct affords a unique opportunity to probe hRFC for ligand-binding domains by cysteine accessibility methods [43,44]. Of particular interest are the residues in or flanking TMD1 (Figure 1B), for which mutations in highly conserved residues (e.g. Gly^{44}, Glu^{45}, Ser^{46} and Ile^{48}) have been reported to result in profound effects on transport substrate binding and/or decreased rates of translocation [18–24].

Twenty-four mutant constructs were prepared from hRFC^{his6} *Cys-less* in which single cysteine residues were introduced from positions 25–48, including the entire predicted TMD1 [48] (Figure 1B). The single-mutant hRFC^{his6} constructs were transfected into transport-impaired MtxRIIOua^{R}2-4 CHO cells and stable transfectants were isolated. A representative Western blot of plasma membrane proteins from stable transfectants expressing the single cysteine-substituted hRFC^{his6} proteins is shown in Figure 4(A). All 24 single cysteine-substituted constructs were expressed in CHO cells and could be detected on Western blots, although the expression levels were variable. For G44C-hRFC^{his6}, a signal could only be detected after an extended exposure to film (shown in Figure 4B).

To assess the effects of the cysteine substitutions on hRFC function, [^{3}H]Mtx uptake was measured for 10 min for each cysteine-substituted hRFC^{his6} mutant. Results are shown in Figure 4(C) as a percentage of the hRFC^{his6} *Cys-less* value and compared with the results from MtxRIIOua^{R}2-4 cells. Most of the cysteine substitutions were remarkably well tolerated, as reflected by the increased uptake over the low level for the MtxRIIOua^{R}2-4 subline. Indeed, of the 24 mutant constructs, only the R42C-hRFC^{his6} was completely inactive (Figure 4C) in spite of high levels of expression on Western blots. Identical results were obtained for additional R42C-hRFC^{his6} clonal isolates (results not

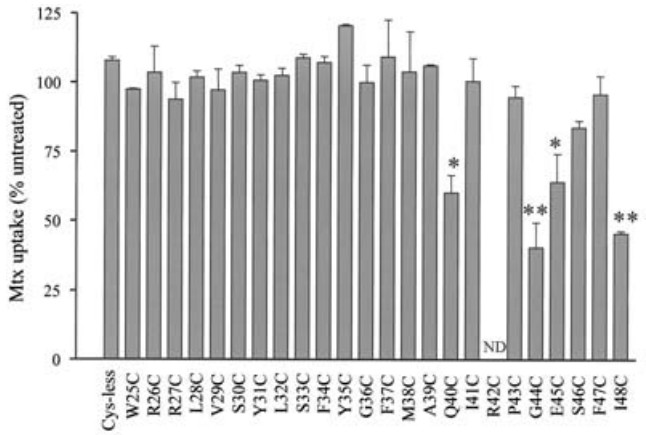

Figure 5 Effects of MTSES treatment on the Mtx uptake by single cysteine-substituted hRFC^{his6} mutants

CHO cells expressing hRFC^{his6} *Cys-less* and single cysteine-substituted hRFC^{his6} mutants were preincubated with and without 1 mM MTSES for 15 min at 37 °C. Cells were washed and 1 μM [^{3}H]Mtx uptake was assayed at 37 °C for 10 min. For each mutant, rates are presented as a percentage of the rate measured in the absence of MTSES. All transport results are expressed as means ± S.E.M. for 2–3 separate experiments. Statistical significance was determined using InStat v. 3 (GraphPad Software, San Diego, CA, U.S.A.). $*P < 0.05$, $**P < 0.01$. ND, not detected.

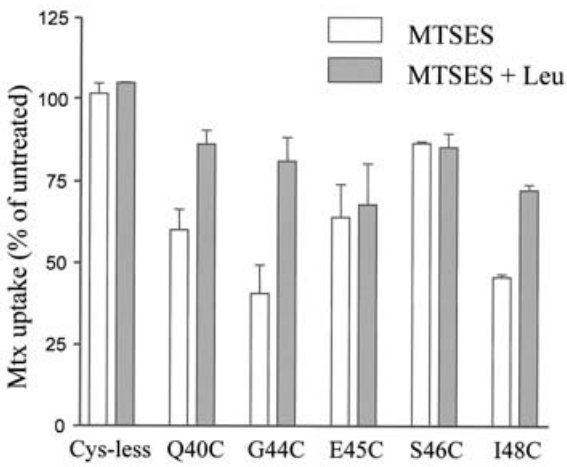

Figure 6 Protection by leucovorin of Q40C-, G44C-, E45C-, S46C- and I48C-hRFC^{his6} mutants from MTSES inhibition

CHO cells expressing hRFC^{his6} *Cys-less* and MTSES-sensitive cysteine substitution mutants were treated with 1 mM MTSES in the presence or absence of 300 μM leucovorin (Leu) before the transport assay. [^{3}H]Mtx (1 μM) uptake was assayed at 37 °C for 10 min. For each mutant, rates are presented as percentages of the rates measured in the absence of MTSES. Results are expressed as means ± S.E.M. for three separate experiments.

shown), suggesting that Arg^{42} may be structurally or functionally important to hRFC transport.

Modification of transport activity of cysteine-substituted hRFC mutants by MTSES

The effects of the small, thiol-reactive alkylthiosulphonate agents, MTSES, MTSEA and MTSET, on Mtx transport by the hRFC^{his6} cysteine mutants should provide an excellent gauge of the aqueous accessibilities of the cysteine substitutions in TMD1. Since Glu^{45} was implicated previously in RFC ligand binding [20–22], the E45C-hRFC^{his6} transfectant was initially used to screen MTSEA, MTSET and MTSES for their capacities to inhibit uptake. E45C-hRFC^{his6} and hRFC^{his6} *Cys-less* cells were treated for 15 min with the methanethiosulphonate (MTS) reagents (2.5 mM, 1 mM and 10 mM respectively) at 37 °C, washed with PBS and assayed for 1 μM [^{3}H]Mtx uptake for 10 min. In this experiment (results not shown), only the negatively charged MTSES inhibited uptake by E45C-hRFC^{his6} without loss of cell viability. MTSEA treatment resulted in a significant loss of cell viability during short exposures, whereas the cationic MTSET was completely inert. In subsequent experiments with Q40C-, G44C- and I48C-hRFC^{his6} mutants, almost identical results were obtained (see below). Neither MTSET nor MTSES inhibited Mtx uptake in the hRFC^{his6} *Cys-less* transfectant. In further experiments, inhibition of E45C-hRFC^{his6} by MTSES showed no effect on increasing concentrations above 1 mM and to exposures longer than 15 min (results not shown).

Figure 5 shows the effects of treating the 24 single cysteine-substituted hRFC^{his6} transfectants with MTSES under the optimized conditions (37 °C, 15 min, 1 mM MTSES) on [^{3}H]Mtx uptake. Since there was no effect on the transport activity of hRFC^{his6} *Cys-less* by MTSES in our preliminary experiments, this was included as a negative control. Of 24 single cysteine mutants analysed, four (Q40C, G44C, E45C and I48C) showed appreciable (>30 %) and statistically significant ($P < 0.05$) losses of activity resulting from MTSES treatment. A small effect (approx. 16 %) was also observed for the S46C-hRFC^{his6} construct.

Notably, 300 μM leucovorin significantly protected Q40C-, G44C- and I48C-hRFC^{his6}-expressing cells from the inhibitory effects of MTSES (Figure 6). These results strongly suggest that amino acids 40, 44 and 48 in hRFC contribute to transport substrate binding.

Mapping the TMD1 extracellular boundary with MTSEA-biotin and biotin maleimide

CHO cells expressing hRFC^{his6} *Cys-less* and cysteine-substituted hRFC^{his6} proteins spanning the predicted TMD1 exofacial boundary (i.e. F37C, M38C, A39C, Q40C, I41C, R42C and P43C; Figure 1B) were treated with membrane-impermeable, thiol-reactive MTSEA-biotin [59] to map the extracellular boundary for TMD. No toxicity was detected. After the treatments, hRFC^{his6} proteins were immunoprecipated with anti-myc antibody and resolved by SDS gels, with detection of surface biotinylated thiols with peroxidase-linked streptavidin. Although all hRFC^{his6} proteins, including both the cysteine-less and cysteine insertion mutants, were effectively immunoprecipitated (Figure 7A), only the P43C, R42C, I41C and Q40C proteins were labelled with MTSEA-biotin (Figure 7B). This establishes their aqueous exposure and accessibility to MTSEA-biotin, reflecting their probable extracellular localization. Conversely, A39C-, M38C- and F37C-hRFC^{his6} proteins were not labelled by MTSEA-biotin, suggesting the inaccessibility of these cysteine residues to thiol modification and probable membrane localization.

To assess the localization of the Gly^{44}, Glu^{45}, Ser^{46} and Ile^{48} residues, found to be functionally important in the present and previous studies [20–24], we treated CHO transfectants expressing the G44C-, E45C-, S46C- and I48C-hRFCs with the surface-labelling reagent biotin maleimide, with and without the membrane-impermeable blocking agent stilbenedisulphonate maleimide [27]. All these positions were effectively labelled with biotin maleimide, and biotinylation was significantly blocked by stilbenedisulphonate maleimide (Figure 8), establishing their extracellular localizations. Conversely, no labelling was detected with biotin maleimide for hRFC^{his6} *Cys-less* (Figure 7B) or for

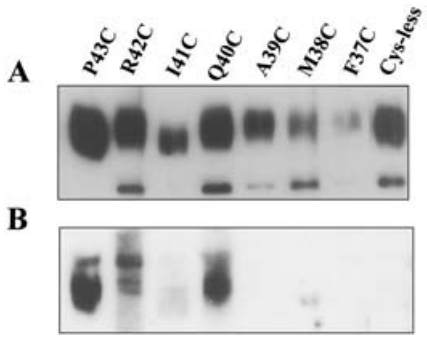

Figure 7 Mapping the TMD1 junction with MTSEA-biotin

CHO cells expressing single cysteine-substituted hRFC^{his6} (positions 37–43) and hRFC^{his6} *Cys-less* were treated with 200 μM MTSEA-biotin, as described in the Materials and methods section. Membrane proteins were immunoprecipitated by anti-myc antibody and Protein G-plus agarose beads, followed by Western blotting. (**A**) Results for total immunoprecipitated hRFC^{his6} protein detected using an hRFC-specific antibody. (**B**) Results for the hRFC^{his6} cysteine mutants labelled with membrane-impermeable MTSEA-biotin and detected using peroxidase-linked streptavidin.

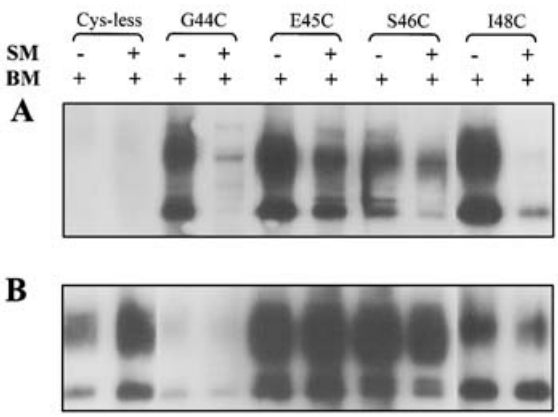

Figure 8 Biotinylation of *Cys-less* and G44C-, E45C-, S46C- and I48C-hRFC^{his6} with biotin maleimide

CHO cells expressing single cysteine-substituted hRFC^{his6} and hRFC^{his6} *Cys-less* proteins were treated with 200 μM biotin maleimide (BM) with or without pretreatment with 200 μM stilbenedisulphonate maleimide (SM). Membrane proteins were immunoprecipitated by anti-myc antibody and Protein G-plus agarose beads, followed by Western blotting. Detection of immunoprecipitated proteins was done with streptavidin peroxidase conjugate (**A**) and hRFC-specific antibody (**B**), after stripping the PVDF membrane with 0.2 M NaOH.

A332C-hRFC^{his6} (located on the cytosolic loop domain connecting TMDs 7 and 8; results not shown).

Collectively, these experiments demonstrate (i) that positions 37–39 are completely inaccessible to membrane-impermeable MTSEA-biotin and the membrane junction lies between positions 39 and 40, and (ii) based on the patterns of biotin maleimide reactivity and protection by stilbenedisulphonate maleimide, amino acids 44–46 and 48 must lie in the exofacial loop connecting TMD1 and TMD2 rather than within TMD1.

DISCUSSION

In the present report, we examined the roles of cysteine residues in the structure and function of hRFC by deleting the C-terminal 56 amino acids, including four cysteine residues, and mutagenizing the remaining seven cysteine residues to serine residues. The initial goals were to assess the importance of cysteine residues to hRFC transport function and, if possible to generate a cysteine-less hRFC construct, to apply cysteine-scanning mutagenesis with thiol-reactive reagents to probe structural/functional features of the native carrier. Our results indicate that substitutions of Cys^{30}, Cys^{33}, Cys^{220}, Cys^{246}, Cys^{365}, Cys^{396} and Cys^{458} with serine residues are well tolerated, as evidenced by the high level of expression and normal plasma membrane targeting of the hRFC^{his6}*Cys-less* protein and by a restoration of the Mtx transport phenotype to transport defective MtxRIIOua^{R}2-4 CHO cells. Essentially identical results were obtained for hRFC^{his6}*Cys-less* expressed in transport-deficient K562 human erythroleukaemia cells (results not shown).

A number of previous reports have identified a number of functionally important residues in the RFC protein from Mtx-resistant mouse or human cell lines [18–24,60]. Of particular interest are highly conserved residues located in or flanking TMD1, for which a disproportionate number of mutations have been localized. For instance, the G44R mutation in hRFC results in a significant increase in the K_t value for Mtx and was first identified in this laboratory in transport-defective CCRF-CEM-Mtx1 cells [18]; G44R was reported most recently in a separate CCRF-CEM subline selected for resistance to PT523 [19]. The E45R mutation was associated with anti-folate resistance and loss of transport in L1210 and CCRF-CEM cells [20–22] and is interesting in that it results in strikingly different effects on the binding of Mtx when compared with either folic acid or leucovorin. Ser^{46} has also been suggested to be important for RFC function, since the S46N mouse RFC mutant results in a decreased rate of carrier mobility, which is greater for Mtx when compared with reduced folates [24]. An S46I mutation in hRFC was also detected in CCRF-CEM cells selected for resistance to the benzoquinazoline anti-folate GW1843U89 [60], and an S46N mutation was detected in a primary osteosarcoma specimen from a patient [61]. Finally, the I48F mutant in mouse RFC results in a selective decrease in the K_t value for folic acid compared with anti-folate substrates (Mtx and Lometrexol) [23].

To further explore the roles of residues in or flanking TMD1 in transport, we inserted single cysteine residues from positions 25–48 in hRFC. All of the single cysteine-substituted hRFC constructs were expressed and, except R42C, were capable of mediating Mtx uptake well above the low level in MtxRIIOua^{R}2–4 cells. Arg^{42} is highly conserved in RFCs from different species and, along with other conserved basic residues (e.g. Arg^{133}, Arg^{373} and Lys^{411} in hRFC), may contribute to the binding of anionic (anti-) folate substrates to the carrier [53,62–64]. In addition, potential interactions with other charged residues similar to that described for Asp^{88} and Arg^{133} in hRFC [53], could contribute to conformational stability required for optimal transport activity.

The 23 functional hRFC^{his6} cysteine mutants were probed with small thiol-reactive MTS reagents and effects on transport activity measured with [^{3}H]Mtx, based on the assumption that the hydrophilic MTS reagents will only react with exposed cysteine residues at water-accessible surfaces (including the putative TMD-spanning 'channel' for translocating folate substrates) and that membrane-buried cysteine residues will be unaffected [43]. Interestingly, in our study, only MTSES was significantly inhibitory without loss of cell viability, whereas MTSEA was cytotoxic and MTSET was completely inactive. This difference between MTSES and MTSET may reflect the binding specificity of hRFC for anionic compounds such as MTSES, whereas the cationic MTSET would probably be excluded from binding. Analogous results were reported by Chan et al. [46] for the effects of MTS reagents on the prostaglandin transporter.

Our results demonstrate that positions 25–39 in hRFC^{his6} were unaffected by MTSES treatments, implying that either these positions were completely inaccessible to the thiol reagent or that their modification by MTSES had no effect on hRFC function. However, other residues were profoundly affected by MTSES treatments, as reflected in statistically significant losses of [^{3}H]Mtx uptake capacity for Q40C-, G44C-, E45C- and I48C-hRFCs and the protection of Q40C-, G44C- and I48C-hRFCs from the effects of MTSES by leucovorin, an established RFC substrate. Although protection by leucovorin from MTSES inhibition could possibly be an indirect consequence of substrate binding distal from this region, based on the mutation data [18–24], we favour a model in which these protected residues participate directly in the transport process.

The lack of protection by leucovorin of E45C-hRFC was surprising in the light of significant effects of amino acid replacements at position 45 on substrate binding [20–22,65], as noted above. However, other amino acid substitutions at position 45, including changes involving charge, size and/or hydrophobicity, preserved at least some level of transport, although this varied with different transport substrates [65]. Collectively, these results imply that the role of Glu^{45} in RFC transport might involve its indirect effect on substrate binding through changes in carrier conformation and/or maintenance of the charge states of residues directly involved in the transport process. Alternatively, the lack of protection from MTSES inhibition by leucovorin could partly reflect a loss of binding of this reduced folate to the E45C mutant carrier.

Although the generalized membrane topology for TMDs 1–7 and the C-terminus of hRFC is now established [66,67] and conforms to that predicted by computer hydropathy analysis [48], the TMD loop boundaries are still uncertain and membrane disposition of Gln^{40}-Ile^{48} peptide has not been confirmed previously. Interestingly, models for RFC secondary structure [68] and membrane topology [48] predict that amino acids 40–48 conform to a random coil rather than an α-helix, and localize to the extracellular face-flanking TMD1 rather than within the membrane-spanning domain (Figure 1B). Consistent with this, our results with membrane-impermeable MTSEA-biotin reagent indicate that the TMD1 exofacial loop boundary lies between Ala^{39} and Gln^{40} and suggest that selective MTSES reactivity towards the Q40C, G44C and I48C mutants is probably due, at least partially, to their surface accessibilities to the MTSES reagent. Importantly, our results indicate that key amino acids (Gly^{44}, Glu^{45}, Ser^{46} and Ile^{48}) suggested previously to be involved in RFC function [18–24] do not contribute to the TMD1 helix. Direct evidence for an exofacial orientation for these residues was provided by biotin maleimide reactivity and stilbenedisulphonate maleimide protection at cysteine residues inserted at these positions. Thus, even though the Gln^{40}-Ile^{48} peptide domain seems to contribute to hRFC transport, this can be envisaged to involve its 'scaffolding' role in binding transport substrates at the exofacial hRFC surface rather than as a structural component of the putative transmembrane channel for folate substrates. Indeed, from the lack of effect of MTSES at cysteine substitutions from positions 25–39 in TMD1, it seems probable that the transmembrane channel comprises TMDs other than TMD1.

Future studies will continue to focus on the identification of key amino acids or domains involved in substrate recognition and membrane translocation, a prerequisite to understanding the molecular mechanism of folate and anti-folate membrane transport by hRFC. This should be greatly facilitated by the availability of an active cysteine-less hRFC, as described in the present study.

We thank our colleagues Dr Xiang Liu and Dr Bee Ching Ding for experimental assistance in preparing the hRFC^{his6} *Cys-less* construct. We also thank Dr Wayne Flintoff for his gift of the MtxRIIOua^{R}2–4 CHO cell line. This study was supported by the National Cancer Institute, National Institutes of Health (grant no. CA53535).

REFERENCES

1 Stokstad, E. L. R. (1990) Historical perspective on key advances in the biochemistry and physiology of folates. In Folic Acid Metabolism in Health and Disease (Picciano, M. F., Stokstad, E. L. R. and Greogory, J. F., eds.), pp. 1–21, Wiley-Liss, New York
2 Mason, J. B. and Levesque, T. (1996) Folate: effects on carcinogenesis and the potential for cancer chemoprevention. Oncology **10**, 1727–1744
3 Butterworth, Jr. C. E. and Bendich, A. (1996) Folic acid and the prevention of birth defects. Annu. Rev. Nutr. **16**, 73–97
4 Refsum, H., Ueland, P. M., Nygard, O. and Vollset, S. E. (1998) Homocysteine and cardiovascular disease. Annu. Rev. Med. **49**, 31–62
5 Whetstine, J. R., Flatley, R. M. and Matherly, L. H. (2002) The human reduced folate carrier gene is ubiquitously and differentially expressed in normal human tissues: identification of seven non-coding exons and characterization of a novel promoter. Biochem. J. **367**, 629–640
6 Sirotnak, F. M. and Tolner, B. (1999) Carrier-mediated membrane transport of folates in mammalian cells. Annu. Rev. Nutr. **19**, 91–122
7 Matherly, L. H. (2001) Molecular and cellular biology of the human reduced folate carrier. Prog. Nucleic Acid Res. Mol. Biol. **67**, 131–162
8 Goldman, I. D. and Matherly, L. H. (1985) The cellular pharmacology of methotrexate. Pharmacol. Ther. **28**, 77–102
9 Sirotnak, F. M. (1985) Obligate genetic expression in tumor cells of a fetal membrane property mediating 'folate' transport: biological significance and implications for improved therapy of human cancer. Cancer Res. **45**, 3992–4000
10 Jansen, G. (1999) Receptor- and carrier-mediated transport systems for folates and antifolates: exploitation for folate-based chemotherapy and immunotherapy. In Antifolate Drugs in Cancer Therapy (Jackman, A. L., ed.), pp. 293–322, Humana Press, Totowa, NJ
11 Zhang, L., Taub, J. W., Williamson, M., Wong, S. C., Hukku, B., Pullen, J., Ravindranath, Y. and Matherly, L. H. (1998) Reduced folate carrier gene expression in childhood acute lymphoblastic leukemia: relationship to immunophenotype and ploidy. Clin. Cancer Res. **4**, 2169–2177
12 Gorlick, R., Cole, P., Banerjee, D., Longo, G., Li, W. W., Hochhauser, D. and Bertino, J. R. (1999) Mechanisms of methotrexate resistance in acute leukemia. Decreased transport and polyglutamylation. Adv. Exp. Med. Biol. **457**, 543–550
13 Guo, W., Healey, J. H., Meyers, P. A., Ladanyi, M., Huvos, A. G., Bertino, J. R. and Gorlick, R. (1999) Mechanisms of methotrexate resistance in osteosarcoma. Clin. Cancer Res. **5**, 621–627
14 Wong, S. C., Proefke, S. A., Bhushan, A. and Matherly, L. H. (1995) Isolation of human cDNAs that restore methotrexate sensitivity and reduced folate carrier activity in methotrexate transport-defective Chinese hamster ovary cells. J. Biol. Chem. **270**, 17468–17475
15 Prasad, P. D., Ramamoorthy, S., Leibach, F. H. and Ganapathy, V. (1995) Molecular cloning of the human placental folate transporter. Biochem. Biophys. Res. Commun. **206**, 681–687
16 Williams, F. M. and Flintoff, W. F. (1995) Isolation of a human cDNA that complements a mutant hamster cell defective in methotrexate uptake. J. Biol. Chem. **270**, 2987–2992
17 Moscow, J. A., Gong, M., He, R., Sgagias, M. K., Dixon, K. H., Anzick, S. L., Meltzer, P. S. and Cowan, K. H. (1995) Isolation of a gene encoding a human reduced folate carrier (RFC1) and analysis of its expression in transport-deficient, methotrexate-resistant human breast cancer cells. Cancer Res. **55**, 3790–3794
18 Wong, S. C., Zhang, L., Witt, T. L., Proefke, S. A., Bhushan, A. and Matherly, L. H. (1999) Impaired membrane transport in methotrexate-resistant CCRF-CEM cells involves early translation termination and increased turnover of a mutant reduced folate carrier. J. Biol. Chem. **274**, 10388–10394
19 Rothem, L., Ifergan, I., Kaufman, Y., Priest, D. G., Jansen, G. and Assaraf, Y. G. (2002) Resistance to multiple novel antifolates is mediated via defective drug transport resulting from clustered mutations in the reduced folate carrier gene in human leukaemia cell lines. Biochem. J. **367**, 741–750
20 Zhao, R., Assaraf, Y. G. and Goldman, I. D. (1998) A mutated murine reduced folate carrier (RFC1) with increased affinity for folic acid, decreased affinity for methotrexate, and an obligatory anion requirement for transport function. J. Biol. Chem. **273**, 19065–19071
21 Jansen, G., Mauritz, R., Drori, S., Sprecher, H., Kathmann, I., Bunni, M., Priest, D. G., Noordhuis, P., Schornagel, J. H., Pinedo, H. M. et al. (1998) A structurally altered human reduced folate carrier with increased folic acid transport mediates a novel mechanism of antifolate resistance. J. Biol. Chem. **273**, 30189–30198
22 Gifford, A. J., Haber, M., Witt, T. L., Whetstine, J. R., Taub, J. W., Matherly, L. H. and Norris, M. D. (2002) Role of the E45K-reduced folate carrier gene mutation in methotrexate resistance in human leukemia cells. Leukemia **16**, 2379–2387

23 Tse, A., Brigle, K., Taylor, S. M. and Moran, R. G. (1998) Mutations in the reduced folate carrier gene which confer dominant resistance to 5,10-dideazatetrahydrofolate. J. Biol. Chem. **273**, 25953–25960

24 Zhao, R., Assaraf, Y. G. and Goldman, I. D. (1998) A reduced folate carrier mutation produces substrate-dependent alterations in carrier mobility in murine leukemia cells and methotrexate resistance with conservation of growth in 5-formyltetrahydrofolate. J. Biol. Chem. **273**, 7873–7879

25 Akabas, M. H., Stauffer, D. A., Xu, M. and Karlin, A. (1992) Acetylcholine receptor channel structure probed in cysteine-substitution mutants. Science **258**, 307–310

26 Javitch, J. A., Li, X., Kaback, J. and Karlin, A. (1994) A cysteine residue in the third membrane-spanning segment of the human D2 dopamine receptor is exposed in the binding-site crevice. Proc. Natl. Acad. Sci. U.S.A. **91**, 10355–10359

27 Loo, T. W. and Clarke, D. M. (1995) Membrane topology of a cysteine-less mutant of human P-glycoprotein. J. Biol. Chem. **270**, 843–848

28 Nicoll, D. A., Ottolia, M., Lu, L., Lu, Y. and Philipson, K. D. (1999) A new topological model of the cardiac sarcolemmal Na^+–Ca^{2+} exchanger. J. Biol. Chem. **274**, 910–917

29 Olsowski, A., Monden, I., Krause, G. and Keller, K. (2000) Cysteine scanning mutagenesis of helices 2 and 7 in GLUT1 identifies an exofacial cleft in both transmembrane segments. Biochemistry **39**, 2469–2474

30 Kimura-Someya, T., Iwaki, S., Konishi, S., Tamura, N., Kubo, Y. and Yamaguchi, A. (2000) Cysteine-scanning mutagenesis around transmembrane segments 1 and 11 and their flanking loop regions of Tn10-encoded metal-tetracycline/H^+ antiporter. J. Biol. Chem. **275**, 18692–18697

31 Hu, Y. K. and Kaplan, J. H. (2000) Site-directed chemical labeling of extracellular loops in a membrane protein. The topology of the Na,K-ATPase α-subunit. J. Biol. Chem. **275**, 19185–19191

32 Qiu, Z., Nicoll, D. A. and Philipson, K. D. (2001) Helix packing of functionally important regions of the cardiac Na^+-Ca^{2+} exchanger. J. Biol. Chem. **276**, 194–199

33 Dodd, J. R. and Christie, D. L. (2001) Cysteine 144 in the third transmembrane domain of the creatine transporter is located close to a substrate-binding site. J. Biol. Chem. **276**, 46983–46988

34 Loo, T. W. and Clarke, D. M. (2000) Identification of residues within the drug-binding domain of the human multidrug resistance P-glycoprotein by cysteine-scanning mutagenesis and reaction with dibromobimane. J. Biol. Chem. **275**, 39272–39278

35 Loo, T. W. and Clarke, D. M. (2001) Defining the drug-binding site in the human multidrug resistance P-glycoprotein using a methanethiosulfonate analog of verapamil, MTS-verapamil. J. Biol. Chem. **276**, 14972–14979

36 Tamura, N., Konishi, S., Iwaki, S., Kimura-Someya, T., Nada, S. and Yamaguchi, A. (2001) Complete cysteine-scanning mutagenesis and site-directed chemical modification of the Tn10-encoded metal-tetracycline/H^+ antiporter. J. Biol. Chem. **276**, 20330–20339

37 Slotboom, D. J., Konings, W. N. and Lolkema, J. S. (2001) Cysteine-scanning mutagenesis reveals a highly amphipathic, pore-lining membrane-spanning helix in the glutamate transporter GltT. J. Biol. Chem. **276**, 10775–10781

38 Stipani, V., Cappello, A. R., Daddabbo, L., Natuzzi, D., Miniero, D. V., Stipani, I. and Palmieri, F. (2001) The mitochondrial oxoglutarate carrier: cysteine-scanning mutagenesis of transmembrane domain IV and sensitivity of Cys mutants to sulfhydryl reagents. Biochemistry **40**, 15805–15810

39 Kwaw, I., Zen, K. C., Hu, Y. and Kaback, H. R. (2001) Site-directed sulfhydryl labeling of the lactose permease of *Escherichia coli*: helices IV and V that contain the major determinants for substrate binding. Biochemistry **40**, 10491–10499

40 Mueckler, M. and Makepeace, C. (2002) Analysis of transmembrane segment 10 of the Glut1 glucose transporter by cysteine-scanning mutagenesis and substituted cysteine accessibility. J. Biol. Chem. **277**, 3498–3503

41 Zeng, F. Y., Hopp, A., Soldner, A. and Wess, J. (1999) Use of a disulfide cross-linking strategy to study muscarinic receptor structure and mechanisms of activation. J. Biol. Chem. **274**, 16629–16640

42 Loo, T. W. and Clarke, D. M. (2001) Determining the dimensions of the drug-binding domain of human P-glycoprotein using thiol cross-linking compounds as molecular rulers. J. Biol. Chem. **276**, 36877–36880

43 Karlin, A. and Akabas, M. H. (1998) Substituted-cysteine accessibility method. Methods Enzymol. **293**, 123–145

44 Loo, T. W. and Clarke, D. M. (1999) Determining the structure and mechanism of the human multidrug resistance P-glycoprotein using cysteine-scanning mutagenesis and thiol-modification techniques. Biochim. Biophys. Acta **1461**, 315–325

45 Frillingos, S., Sahin-Toth, M., Wu, J. and Kaback, H. R. (1998) Cys-scanning mutagenesis: a novel approach to structure function relationships in polytopic membrane proteins. FASEB J. **12**, 1281–1299

46 Chan, B. S., Satriano, J. A. and Schuster, V. A. (1999) Mapping the substrate binding site of the prostaglandin transporter PGT by cysteine scanning mutagenesis. J. Biol. Chem. **274**, 25564–25570

47 Ferrer, J. V. and Javitch, J. A. (1998) Cocaine alters the accessibility of endogenous cysteines in putative extracellular and intracellular loops of the human dopamine transporter. Proc. Natl. Acad. Sci. U.S.A. **95**, 9238–9543

48 Hofmann, K. and Stoffel, W. (1993) TMBASE – a database of membrane spanning protein segments. Biol. Chem. Hoppe-Seyler **374**, 166

49 Goldman, I. D., Lichtenstein, N. S. and Oliverio, V. T. (1968) Carrier-mediated transport of the folic acid analogue, methotrexate, in the L1210 leukemia cell. J. Biol. Chem. **243**, 5007–5017

50 Fry, D. W., Yalowich, J. C. and Goldman, I. D. (1982) Rapid formation of poly-γ-glutamyl derivatives of methotrexate and their association with dihydrofolate reductase as assessed by high pressure liquid chromatography in the Ehrlich ascites tumor cell *in vitro*. J. Biol. Chem. **257**, 1890–1896

51 Flintoff, W. F., Davidson, S. V. and Siminovitch, L. (1976) Isolation and partial characterization of three methotrexate-resistant phenotypes from Chinese hamster ovary cells. Somatic Cell Genet. **2**, 245–261

52 Horton, R. M., Cai, Z. L., Ho, S. N. and Pease, L. R. (1990) Gene splicing by overlap extension: tailor-made genes using the polymerase chain reaction. Biotechniques **8**, 528–535

53 Liu, X. Y. and Matherly, L. H. (2001) Functional interactions between arginine-133 and aspartate-88 in the human reduced folate carrier: evidence for a charge-pair association. Biochem. J. **358**, 511–516

54 Matherly, L. H., Czajkowski, C. A. and Angeles, S. M. (1991) Identification of a highly glycosylated methotrexate membrane carrier in K562 human erythroleukemia cells up-regulated for tetrahydrofolate cofactor and methotrexate transport. Cancer Res. **51**, 3420–3426

55 Laemmli, U. K. (1970) Cleavage of structural proteins during the assembly of the head of bacteriophage T4. Nature (London) **227**, 680–685

56 Matsudaira, P. (1987) Sequence from picomole quantities of proteins electroblotted onto polyvinylidene difluoride membranes. J. Biol. Chem. **262**, 10035–10038

57 Lowry, O. H., Rosebrough, N. J., Farr, A. L. and Randall, R. J. (1951) Protein measurement with the Folin phenol reagent. J. Biol. Chem. **193**, 265–275

58 Wong, S. C., McQuade, R., Proefke, S. A., Bhushan, A. and Matherly, L. H. (1997) Human K562 transfectants expressing high levels of reduced folate carrier but exhibiting low transport activity. Biochem. Pharmacol. **53**, 199–206

59 Hu, Y. K. and Kaplan, J. H. (2000) Site-directed chemical labeling of extracellular loops in a membrane protein. The topology of the Na,K-ATPase subunit. J. Biol. Chem. **275**, 19185–19191

60 Drori, S., Jansen, G., Mauritz, R., Peters, G. J. and Assaraf, Y. G. (2000) Clustering of mutations in the first transmembrane domain of the human reduced folate carrier in GW1843U89-resistant leukemia cells with impaired antifolate transport and augmented folate uptake. J. Biol. Chem. **275**, 30855–30863

61 Yang, R., Sowers, R., Mazza, B., Healey, J. H., Huvos, A., Grier, H., Bernstein, M., Beardsley, G. P., Krailo, M. D., Devidas, M. et al. (2003) Sequence alterations in the reduced folate carrier are observed in osteosarcoma tumor samples. Clin. Cancer Res. **9**, 837–844

62 Sharina, I. G., Zhao, R., Wang, Y., Babani, S. and Goldman, I. D. (2001) Mutational analysis of the functional role of conserved arginine and lysine residues in transmembrane domains of the murine reduced folate carrier. Mol. Pharmacol. **59**, 1022–1028

63 Witt, T. L. and Matherly, L. H. (2002) Identification of lysine-411 in the human reduced folate carrier as an important determinant of substrate selectivity and carrier function by systematic site directed mutagenesis. Biochim. Biophys. Acta **1567**, 56–62

64 Sadlish, H., Williams, F. M. and Flintoff, W. F. (2002) Functional role of arginine 373 in substrate translocation by the reduced folate carrier. J. Biol. Chem. **277**, 42105–42112

65 Zhao, R., Gao, F., Wang, P. J. and Goldman, I. D. (2000) Role of the amino acid 45 residue in reduced folate carrier function and ion-dependent transport as characterized by site-directed mutagenesis. Mol. Pharmacol. **57**, 317–323

66 Liu, X. Y. and Matherly, L. H. (2002) Analysis of membrane topology of the human reduced folate carrier protein by hemagglutinin epitope insertion and scanning glycosylation insertion mutagenesis. Biochim. Biophys. Acta **1564**, 333–342

67 Ferguson, P. L. and Flintoff, W. F. (1999) Topological and functional analysis of the human reduced folate carrier by hemagglutinin epitope insertion. J. Biol. Chem. **274**, 16269–16278

68 Combet, C., Blanchet, C., Geourjon, C. and Deleage, G. (2000) NPS@: network protein sequence analysis. TIBS **25**, 147–150

Received 24 February 2003/5 May 2003; accepted 16 May 2003
Published as BJ Immediate Publication 16 May 2003, DOI 10.1042/BJ20030301